11304 *Biochemistry* **2009,** *48,* 11304–11311
DOI: 10.1021/bi901496q

BIOCHEMISTRY
including biophysical chemistry & molecular biology
Article

Dynamics and Energetics of the Base Flipping Conformation Studied with Base Pair-Mimic Nucleosides[†]

Shu-ichi Nakano,*[,‡,§] Hirohito Oka,[‖] Yuuki Uotani,[‖] Kazuya Uenishi,[⊥] Masayuki Fujii,[⊥,@] and Naoki Sugimoto*[,‡,§,‖]

[‡]*Faculty of Frontiers of Innovative Research in Science and Technology (FIRST) and* [§]*Frontier Institute for Biomolecular Engineering Research (FIBER) and* [‖]*Department of Chemistry, Faculty of Science and Engineering and Konan University, 7-1-20, Minatojima-minamimachi, Chuo-ku, Kobe 650-0047, Japan,* [⊥]*Molecular Engineering Institute (MEI) and* [@]*Department of Environmental and Biological Chemistry, Kinki University, 11-6 Kayanomori, Iizuka, Fukuoka 820-8555, Japan*

Received August 26, 2009; Revised Manuscript Received October 2, 2009

ABSTRACT: A base flipping conformation is found in many biological processes, including DNA repair and DNA and RNA modification processes. To investigate the dynamics and energetics of this unusual conformation in a double helix, base flipping induced by the base pair analogues of deoxyadenosine and deoxycytidine derivatives tethering a phenyl or naphthyl group was investigated. DNA strands bearing the base pair analogues stabilized the base flipping conformation of a complementary RNA, resulting in a site-specific hydrolysis by specific base catalysis. Measurements of the hydrolysis rate and the thermal stability of DNA/RNA duplexes suggested an unconstrained flexibility of the flipped-out ribonucleotide. As established in the base flipping by DNA repair and DNA and RNA modification enzymes, the results suggested that base flipping occurred in competition with base pair formation. In addition, the deoxycytidine derivatives discriminated G from I (inosine), with respect to the base pair interaction energy, as observed for a damaged base or a weakened base pair search by DNA repair proteins. The base pair mimic nucleosides would be useful for investigating the base flipping conformation under the equilibrium with base pairing.

Stacking interactions between nucleotide bases are important for the integrity and stabilization of the double-helical structure of DNA and RNA, while interbase hydrogen bonds play a central role in pairing between nucleotide bases. The stacking energy, which was obtained from a dangling end study and an abasic nucleotide analogue study, is in the range of 0.5−1.8 kcal mol^{-1} (1 kcal = 4.18 kJ) in $-\Delta G°_{37}$[1] (*1*−*4*). Disruptions of the continuous stacking occur due to an abasic site and a flipped-out base in a double helix. An abasic site is a naturally occurring apurinic/apyrimidinic (AP) site as a result of DNA damage. The base flipping conformation is formed by moving a nucleotide base from a base-stacked position to an extrahelical position, accompanied by backbone distortion. This conformation is generated as an intermediate in the DNA repair and DNA and RNA modification pathways (*5*−*7*). These unusual conformations largely decrease the stability of the duplex and are thermodynamically very unstable. An abasic analogue, such as tetrahydrofuran, can be used for the study of the abasic site, and the thermodynamic stability and dynamics of an AP site-containing duplex have been well studied (*8*−*10*). On the other hand, it is difficult to investigate the base flipping in experiments because the conformation can be formed only after overcoming the interaction energy of the intrahelical base stacking or base pairing.

The base flipping conformation is stabilized by interactions with proteins. For example, uracil DNA glycosylase recognizes an oxidized cytosine lesion and the damaged base is flipped out of the helix into the enzyme active site and amino acid residues are inserted into the DNA helix (*11*). DNA and RNA modification enzymes, including DNA methyltransferase and RNA adenosine deaminase, also assist the base flipping conformation to reach their target base (*6*, *7*). A base flipping conformation can also be generated using an artificial nucleoside bearing a strong stacking group. Compounds with an extended π-system of a planar aromatic ring, such as nucleoside analogues of a pyrene nucleoside and a porphyrin nucleoside incorporated near the center of a duplex, stack into a DNA duplex but significantly perturb the helical structure because of their very large stacking area and a lack of base pairing ability (*12*−*16*). We have examined a deoxyadenosine derivative tethering the phenyl group at *N*6 of deoxyadenosine by a ureido linker, namely A^{phe} (Figure 1A), as an A/T or A/U base pair analogue, and found that A^{phe} located in the center of a DNA sequence did not perturb the global duplex conformation but induced base flipping in a complementary strand by intercalating the phenyl group into the helix (*17*).

[†]This work was supported in part by Grants-in-Aid for Scientific Research, the "Core Research" Project (2009−2014) and the "Academic Frontier" Project (2004−2009) from the Ministry of Education, Culture, Sports, Science and Technology, Japan, and the Hirao Taro Foundation of the Konan University Association for Academic Research.

*To whom correspondence should be addressed. E-mail: shuichi@center.konan-u.ac.jp or sugimoto@konan-u.ac.jp. Phone: +81-78-303-1429. Fax: +81-78-303-1495.

[1]Abbreviations: A^{naph}, *N*6-(*N*′-naphthylcarbamoyl)-2′-deoxyadenosine; AP site, apurinic/apyrimidinic site; A^{phe}, *N*6-(*N*′-phenylcarbamoyl)-2′-deoxyadenosine; C^{naph}, *N*6-(*N*′-naphthylcarbamoyl)-2′-deoxycytidine; C^{phe}, *N*6-(*N*′-phenylcarbamoyl)-2′-deoxycytidine; EDTA, ethylenediaminetetraacetic acid; ESI, electrospray ionization; 6-FAM, 6-carboxylfluorescein; $\Delta G°_{37}$, change in the Gibbs free energy at 37 °C; HEPES, 4-(2-hydroxyethyl)-1-piperazineethanesulfonic acid; HPLC, high-performance liquid chromatography; I, inosine; MALDI-TOF, matrix-assisted laser desorption ionization time-of-flight; NMR, nuclear magnetic resonance; PAGE, polyacrylamide gel electrophoresis; pK_a, negative logarithm of the acid dissociation constant; T_m, melting temperature; Tris-HCl, 2-amino-2-(hydroxymethyl)-1,3-propanediol hydrochloride; UV, ultraviolet.

 Published on Web 10/19/2009

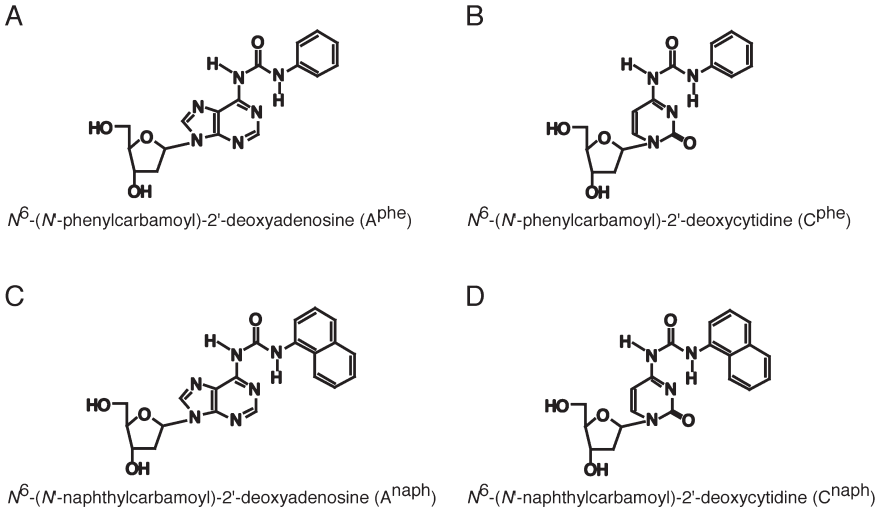

FIGURE 1: Chemical structures of the base pair analogues of deoxyadenosine and deoxycytidine derivatives.

The base flipping induced by A^{phe} induces a site-selective hydrolysis of a complementary RNA sequence (*18*). In this study, the hydrolysis is used to investigate the conformation and dynamics of the flipped-out ribonucleotide. The base flipping conformation is stabilized by the deoxyadenosine and deoxycytidine derivatives, designed as the base pair analogue of A/U and C/G, respectively. Measurements of the RNA hydrolysis rate and duplex stability indicate that the flipped-out nucleotides have an exposed backbone conformation and a significant loss in the level of base stacking. In addition, since the base pair analogues retain a nucleotide base moiety for base pairing with U or G (Figure 1), the base flipping conformation is equilibrated with the base pair conformation, which can be a model of the base flipping by enzymes.

MATERIALS AND METHODS

Oligonucleotide Syntheses. Synthesis of a phosphoramidite of deoxycytidine derivatives tethering the phenyl or naphthyl group was started from 2′-deoxycytidine, as performed for the synthesis of deoxyadenosine derivatives that started from 2′-deoxyadenosine (*17*). All chemicals were purchased either from Aldrich or from Wako Chemicals, and the solvents were freshly distilled prior to use. ^{1}H NMR spectra (Varian INOVA 400 NMR spectrometer) and ESI mass spectra (Finnigan Mat LCQ mass spectrometer) were used to identify compounds.

DNA oligomers containing the base pair analogue and RNA oligomers labeled with 6-carboxylfluorescein (6-FAM) at the 5′-end were synthesized on a solid support by phosphoramidite chemistry using an automated DNA synthesizer (Applied Biosystems model 391). The samples were purified by reverse-phase HPLC on a C18 column (Tosoh) or polyacrylamide gel electrophoresis (PAGE) including 7 M urea after the removal of protecting groups, followed by desalting with a C18 cartridge column. The molecular weight of a DNA strand containing a base pair analogue was determined by MALDI-TOF mass spectra (PE Biosystems Voyager DE). Unmodified DNAs of HPLC purification grade were purchased from Hokkaido System Science, and their molecular weights were determined by MALDI-TOF mass spectra.

Nonenzymatic Hydrolysis of RNA. We prepared DNA/RNA hybrid duplexes of d(GTGTC$\underline{W}_1$CTGTC)/r(GACAG$\underline{W}_2$GACAC) by forming a W_1/W_2 pair in the center of a double helix. A mixture containing 10 μM RNA and 20 μM DNA in a buffer consisting of 20 mM HEPES and 0.13 mM Na_2EDTA (pH 8.0) was incubated at 60 °C for 2 min prior to use. After incubation at 37 °C for 10 min, nonenzymatic hydrolysis of the RNA strand was initiated via addition of an appropriate metal ion and stopped via addition of a 3-fold excess volume of a solution containing 20 mM Na_2EDTA and 7 M urea. To monitor the hydrolysis reaction, gel electrophoresis was performed using a 20% polyacrylamide gel containing 7 M urea in a 1× TBE buffer containing 0.1 M Tris-HCl, 83 mM boric acid, and 1 mM Na_2EDTA (pH 8.3).

Fluorescence from 6-FAM on the RNA strand was visualized and quantified by a fluorescent scanner using a 473 nm excitation laser and a 520 nm emission filter (Fujifilm FLA-5100). RNA hydrolysis experiments were performed in two or three independent trials, and the amounts of hydrolyzed fragments were taken from an average of those obtained independently. The rate constant for hydrolysis was calculated from the time-dependent hydrolyzed yield fit to a linear regression equation.

UV Melting Curve of a DNA/RNA Duplex. UV absorbance was measured by a spectrophotometer (Shimadzu 1700) equipped with a temperature controller. The melting curve was monitored at a heating rate of 0.5 °C min^{-1} and 260 nm in a buffer containing 1 M NaCl, 10 mM Na_2HPO_4, and 1 mM Na_2EDTA (pH 7.0). The extinction coefficient of an oligonucleotide was calculated on the basis of the nearest-neighbor approximation (*19*), and the extinction coefficients of deoxyadenosine and deoxycytidine derivatives were assumed to be the same as those of deoxyadenosine and deoxycytidine, respectively. The melting temperature (T_m), at which half of the nucleotide strands were in a duplex state and half were in a single-stranded state, was estimated from the melting curve obtained using the total nucleotide strand concentration of 20 μM (*20*, *21*).

RESULTS

Site-Selective RNA Hydrolysis Induced by Metal Ions. Deoxyadenosine and deoxycytidine derivatives, designed as a base pair mimic compound, contain the phenyl or naphthyl group tethered to the amino group on a nucleotide base moiety by a ureido linker (Figure 1). The compounds can form a base pair in accordance with the Watson−Crick base pairing rule when the aromatic hydrocarbon group is oriented outside the helix. Instead, the aromatic hydrocarbon group stacks into a double helix when intercalating into a helix and adopts a stacking geometry similar to that of Watson−Crick base pairs. When a

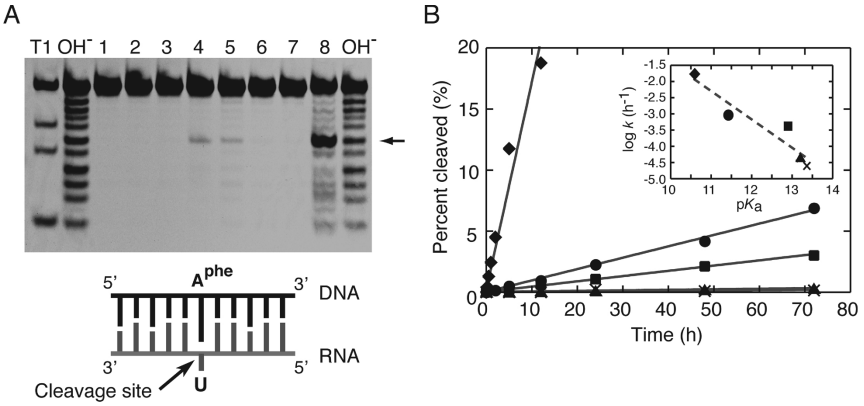

FIGURE 2: (A) PAGE image of the hydrolysis of r(GACAGUGACAC) labeled with fluorescein (6-FAM) at the 5′-end associated with the complementary DNA of d(GTGTCA^{phe}CTGTC). The reaction was performed for 12 h at pH 8.0 and 37 °C in the absence and presence of a metal ion (lane 1, no metal ion added; lane 2, 1 M NaCl; lane 3, 10 mM $[Co(NH_3)_6]Cl_3$; lane 4, 10 mM $MgCl_2$; lane 5, 10 mM $CaCl_2$; lane 6, 10 mM $BaCl_2$; lane 7, 10 mM $SrCl_2$; and lane 8, 10 mM $MnCl_2$). Marker lanes (OH^- lane, alkaline hydrolysis ladder of the RNA; and T1 lane, RNA fragments digested by ribonuclease T1 showing the position of G on the RNA strand) were also used in the same polyacrylamide gel. The arrowhead indicates the cleaved RNA fragment six nucleotides in length. (B) Amounts of cleaved RNA were plotted vs time in the presence of 10 mM $MgCl_2$ (●), $CaCl_2$ (■), $BaCl_2$ (▲), $SrCl_2$ (×), or $MnCl_2$ (◆). The relationship between the logarithm of the rate constant (log k) for the hydrolysis and the pK_a of the metal ion is given in the inset.

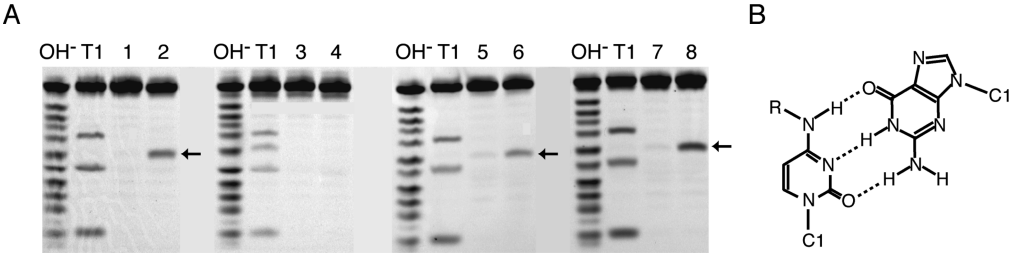

FIGURE 3: (A) PAGE image of the hydrolysis of r(GACAGW$_2$GACAC) (W$_2$ is A in lanes 1 and 2, G in lanes 3 and 4, C in lanes 5 and 6, or U in lanes 7 and 8) associated with d(GTGTCW$_1$CTGTC) (W$_1$ is C in lanes 1, 3, 5, and 7, and W$_1$ is C^{phe} in lanes 2, 4, 6, and 8) perfomred with 10 mM $MgCl_2$ at pH 8.0 and 37 °C for 12 h. The arrowhead indicates the cleaved RNA fragment six nucleotides in length. Two marker lanes of OH^- and T1 were examined for each RNA sequence. (B) Structure of the G/C^{phe} base pair through hydrogen bonds. C1 and R represent the furanose sugar carbon and the phenylcarbamoyl group, respectively.

DNA oligonucleotide bearing a base pair analogue hybridizes with a complementary RNA sequence, an intercalation of the aromatic group into the double helix forces the opposite ribonucleotide base to an extrahelical position, causing the phosphodiester linkage to be susceptible to hydrolysis.

Figure 2A shows the PAGE image for the hydrolysis of RNA r(GACAGUGACAC) labeled with fluorescein at the 5′-end. The RNA strand associated with the complementary DNA of d(GTGTCA^{phe}CTGTC) was incubated in the absence or presence of NaCl, $[Co(NH_3)_6]Cl_3$, $MgCl_2$, $CaCl_2$, $BaCl_2$, $SrCl_2$, or $MnCl_2$ at pH 8.0 and 37 °C. Although NaCl and $[Co(NH_3)_6]Cl_3$ provided no cleaved product, a six-nucleotide length corresponding to RNA strand scission at the 3′-end of U opposite A^{phe} was obtained with $MgCl_2$ and $CaCl_2$, and a large amount of the cleaved fragment was obtained with $MnCl_2$. The hydrolysis data indicated a base flipping conformation and a lack of base pairing between U and the adenine moiety on A^{phe}. Time-dependent reaction yields revealed that the amount of cleaved fragment linearly increased with reaction time, and the reaction rate responsible for the slope differed among alkali earth metal ions and manganese ion (Figure 2B). The negative linear correlation with a slope of −0.88 between the rate constant data and the pK_a values of metal ions (see the inset of Figure 2B) suggests that RNA hydrolysis is catalyzed by a metal-bound hydroxide ion (*22*, *23*).

Examinations of the DNA Strand Bearing C^{phe}. As observed with A^{phe}, DNA/RNA duplexes containing C^{phe} tethering the phenyl group at *N*4 of deoxycytidine (Figure 1B) produced a cleaved RNA fragment in the presence of $MgCl_2$. Comparisons of the electrophoretic mobility of the cleaved fragment in the polyacrylamide gel to those of the alkali hydrolysis ladder and the RNA fragments digested by ribonuclease T1 verified an exclusive hydrolysis at the 3′-end of A, C, or U opposite C^{phe} (Figure 3A). The site-selective reaction indicates base flipping of the ribonucleotide opposite C^{phe} in the duplex. In contrast, no cleaved product was observed when G was located opposite C^{phe}. These data suggest C^{phe}/G base pairing by orienting the phenyl group outside the helix (Figure 3B).

For a convenient measure of the DNA/RNA duplex stability, the thermal melting temperature (T_m) of the d(GTGTCW$_1$CTGTC)/r(GACAGW$_2$GACAC) duplexes (W$_1$ is A, C, or the base pair analogue, and W$_2$ is A, G, C, or U) was measured in a buffer containing 1 M NaCl instead of $MgCl_2$ to prevent RNA hydrolysis (Figure S1 of the Supporting Information and Table 1). The DNA/RNA duplexes forming the A/U or C/G base pair at W$_1$/W$_2$ exhibited higher T_m values (63.0 and 70.8 °C, respectively), and those containing unmodified mismatch pairs (A/A, A/G, A/C, C/A, C/C, and C/U) exhibited lower T_m values ranging from 47.8 to 55.7 °C reflecting different mismatch interactions, as determined in a previous study (*21*). However, T_m values of the duplexes containing A^{phe} (W$_1$ is A^{phe}) were similar to each other regardless of the W$_2$ type (53.4−52.4 °C). The duplexes containing C^{phe} (W$_1$ is C^{phe}) also exhibited similar

Table 1: T_m Values (°C) of DNA/RNA d(GTGTC$\underline{W_1}$CTGTC)/r(GACAG$\underline{W_2}$GACAC) Duplexes Measured in a Buffer Containing 1 M NaCl[a]

W_1	W_2 = A	W_2 = G	W_2 = C	W_2 = U
A	50.1	55.7	51.1	63.0
A^{phe}	53.2	52.9	52.4	52.6
A^{naph}	55.4 (2.2)	55.6 (2.7)	57.0 (4.6)	57.4 (4.8)
C	52.0	70.8	47.8	49.4
C^{phe}	55.2	64.3	56.2	56.1
C^{naph}	58.3 (3.1)	62.3 (−2.0)	60.7 (4.5)	60.2 (4.1)

[a] T_m was measured at a total strand concentration of 20 μM. The values when W_1 is A and A^{phe} were derived from our previous study (*18*). The values in parentheses are the differences in the T_m values resulting from a change in the phenyl group to the naphthyl group on the base pair analogues.

T_m values of 55.2 (W_2 is A), 56.2 (W_2 is C), and 56.1 °C (W_2 is U). The similarity in the T_m values of different RNA sequences corresponds with the W_2 base flipping at an extrahelical position where the base stacking interaction is less significant. In contrast, the T_m of the DNA/RNA duplex containing the C^{phe}/G pair was 64.3 °C, which is much higher than the value of that containing C^{phe}/A, C^{phe}/C, and C^{phe}/U pairs, and is consistent with the formation of the C^{phe}/G base pair through hydrogen bonds.

Comparisons of RNA Hydrolysis Rates and Duplex Stabilities. To assess the degree of ribonucleotide base flipping, the RNA hydrolysis rate was obtained from time-dependent product yields (Figure S2 of the Supporting Information). Table 2 summarizes the rate constant data at 10 mM $MgCl_2$ and indicates similar hydrolysis rates regardless of the ribonucleotide type opposite A^{phe} ($0.71-1.3 \times 10^{-3}$ h^{-1}). The duplexes containing C^{phe}/A, C^{phe}/C, and C^{phe}/U pairs also exhibited reaction rates similar to each other ($2.1-3.6 \times 10^{-3}$ h^{-1}), except for the C^{phe}/G pair indicating no reaction. Although the RNA hydrolysis induced by A^{phe} or C^{phe} was relatively slow (5−26% cleavage yield after a 72 h reaction), the reaction was substantial in comparison with those of the unmodified duplexes containing a mismatched W_1/W_2 pair [< 1% yield after 72 h (data not shown)]. Notably, RNA hydrolysis exclusively occurred on the ribonucleotide opposite A^{phe} or C^{phe}, and no other hydrolyzed fragment was detected.

The base pair analogues of A^{naph} (Figure 1C) and C^{naph} (Figure 1D) tethering the naphthyl group were further examined. More efficient RNA hydrolysis is expected if the naphthyl group of a larger stacking area intercalates more efficiently into a DNA/RNA duplex. Substitution of the naphthyl group for the phenyl group on deoxyadenosine increased the T_m by 2.2−4.8 °C (Table 1), indicating a stronger interaction with A^{naph} than A^{phe}. Changes in the T_m by 3.1−4.5 °C were also observed with substitution of C^{naph} for C^{phe} opposite A, C, or U. However, the data in Table 2 show similar reaction rates between A^{phe} and A^{naph} ($0.71-1.5 \times 10^{-3}$ h^{-1}) and between C^{phe} and C^{naph} ($1.5-3.6 \times 10^{-3}$ h^{-1}). This observation suggests that the perturbations of the ribonucleotide conformation by the phenyl group are as efficient as that by the naphthyl group. It is noteworthy that a small amount of the RNA fragment cleaved on the G opposite C^{naph} was obtained (3% yield after 72 h); however, a predominant base pair conformation is evident from a reaction yield smaller than those for the duplexes containing the C^{naph}/A, C^{naph}/C, and C^{naph}/U pairs [12−20% yield after 72 h (shown in Figure S2 of the Supporting Information)].

Table 2: Rate Constants of RNA Hydrolysis (10^{-3} h^{-1}) at the 3′-End of W_2 in the d(GTGTC$\underline{W_1}$CTGTC)/r(GACAG$\underline{W_2}$GACAC) Duplex in the Presence of 10 mM $MgCl_2$ at pH 8.0 and 37 °C[a]

W_1	W_2 = A	W_2 = G	W_2 = C	W_2 = U
A	< 0.1	< 0.1	< 0.1	< 0.1
A^{phe}	0.71	1.2	1.3	0.94
A^{naph}	1.4	1.5	1.4	1.3
C	< 0.1	< 0.1	0.1	< 0.1
C^{phe}	3.0	< 0.1	2.1	3.6
C^{naph}	2.2	0.4	1.5	2.7

[a] The error values are within 3%. Reaction yields of < 0.5% after the 72 h reaction are represented by < 0.1.

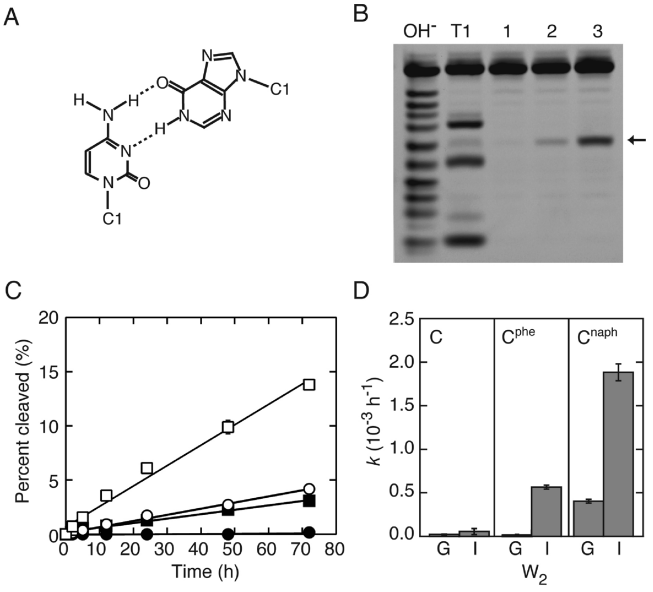

FIGURE 4: (A) C/I base pair through hydrogen bonds. (B) PAGE image of the hydrolysis of r(GACAGIGACAC) associated with d(GTGTC$\underline{W_1}$CTGTC) (lane 1, W_1 = C; lane 2, W_1 = C^{phe}; and lane 3, W_1 = C^{naph}) for 12 h in the presence of 10 mM $MgCl_2$ at pH 8.0 and 37 °C. The arrowhead indicates the cleaved RNA fragment six nucleotides in length. (C) Amounts of cleaved RNA for the duplexes containing the C^{phe}/G (●), C^{naph}/G (■), C^{phe}/I (○), or C^{naph}/I (□) pair plotted versus time. (D) Comparison of the rate constants for the hydrolysis of r(GACAG$\underline{W_2}$GACAC) (W_2 = G or I) associated with d(GTGTC$\underline{C}$CTGTC), d(GTGTC$\underline{C^{phe}}$CTGTC), or d(GTGTC$\underline{C^{naph}}$CTGTC).

Modulation of Base Pair Stability. RNA hydrolysis and the T_m data indicate different results regarding the base pairing ability for deoxyadenosine and deoxycytidine derivatives; C^{phe} and C^{naph} exhibited their base pairing ability, but A^{phe} and A^{naph} exhibited no ability to pair with U. Since the C/G base pair is stronger than the A/U base pair, the influence of base pair stability on the ribonucleotide conformation was investigated using an RNA strand containing inosine (I). The ribonucleotide residue of I has an ability to form a base pair with cytosine through two hydrogen bonds, as demonstrated in Figure 4A. The T_m of a duplex containing the C/I pair was 65.0 °C, which was lower than that containing the C/G base pair (70.8 °C), but was significantly higher than the T_m values of those containing an unmodified C/A, C/C, or C/U mismatch pair (47.8−52.0 °C). Figure 4B demonstrates hydrolysis of an RNA strand containing I opposite C, C^{phe}, or C^{naph}. No cleaved band on I opposite C was observed, in agreement with the base pairing. In contrast, C^{naph} efficiently induced RNA cleavage, and C^{phe} provided a small

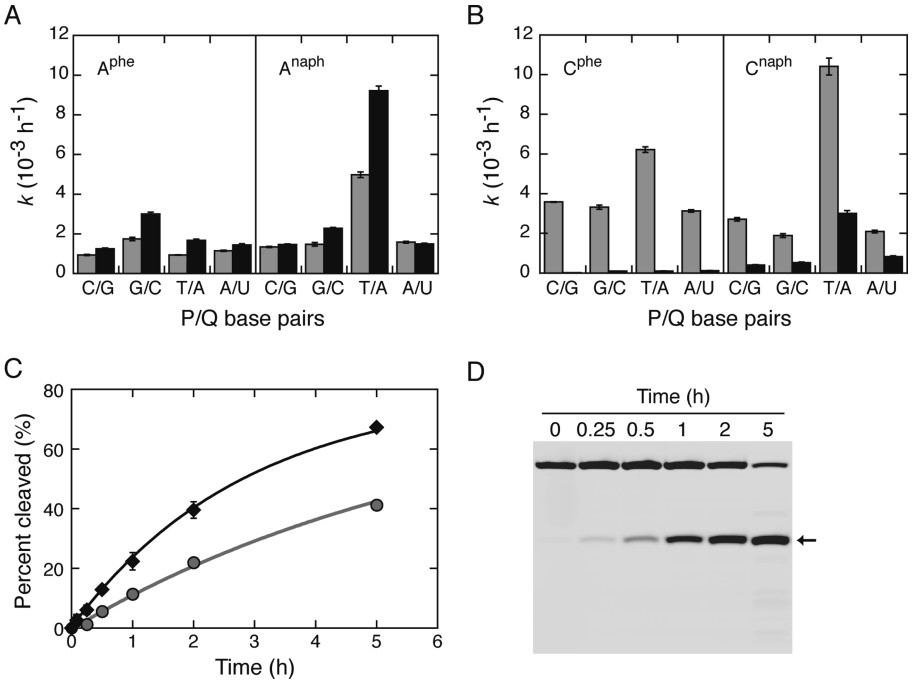

FIGURE 5: (A and B) Comparisons of RNA hydrolysis rates of r(GACAQW_2QACAC) [W_2 = U (gray) or G (black)] associated with d(GTGTPW_1PTGTC) [W_1 = A^{phe} or A^{naph} (A), and W_1 = C^{phe} or C^{naph} (B)] in the presence of 10 mM $MgCl_2$ at pH 8.0 and 37 °C. (C) Kinetic traces for the hydrolysis of r(GACAAUAACAC) associated with d(GTGTTC^{naph}TTGTC) (black) and r(GACAAGAACAC) associated with d(GTGTTA^{naph}TTGTC) (gray) in the presence of 10 mM $MnCl_2$ at pH 8.0 and 37 °C. (D) PAGE image of the hydrolysis of r(GACAAUAACAC) associated with d(GTGTTC^{naph}TTGTC) in the presence of 10 mM $MnCl_2$.

amount of the cleaved fragment. The hydrolyses for C^{phe}/I and C^{naph}/I pairs were much faster than those for C^{phe}/G and C^{naph}/G pairs (Figure 4C,D), and the rate constant for the C^{naph}/I pair was comparable to that for the A^{naph}/U pair.

Influence of Adjacent Base Pairs. These studies used DNA sequences containing a base pair analogue adjacent to cytidine on both sides, thus forming a CW_1C/GW_2G trinucleotide in the center of a DNA/RNA duplex. Because the adjacent base pair influences the stacking interaction of the W_1/W_2 pair, we also examined different trinucleotide sequences (GW_1G/CW_2C, TW_1T/AW_2A, and AW_1A/UW_2U). The duplex stability changed in a trinucleotide sequence-dependent manner (Table S1 of the Supporting Information), and the influence of the trinucleotide sequence on duplex stability was more significant than when I was substituted for G in the RNA strand.

RNA hydrolysis experiments were performed in the presence of 10 mM $MgCl_2$, and similar kinetic data were obtained with the DNA strands bearing A^{phe} or A^{naph}, regardless of the opposite ribonucleotide being U or G (Figure 5A). These results support perturbations of the intrahelical stacking of U and G in a similar degree and an inability to form a base pair between U and deoxyadenosine derivatives. A weak influence of the adjacent base pair type on the hydrolysis rate was observed, the exception being that the TA^{naph}T/AW_2A trinucleotide exhibited a somewhat faster rate. No substantial hydrolysis on G opposite C^{phe} and a small amount of the RNA fragment cleaved on G opposite C^{naph} were observed even when the adjacent base pairs were changed from C/G to G/C, T/A, or A/U (Figures 5B and S3). The U residue opposite C^{phe} or C^{naph} was efficiently cleaved; the duplexes forming a TC^{naph}T/AUA trinucleotide exhibited a higher rate constant of approximately 1×10^{-2} h^{-1}, while the corresponding unmodified duplex forming a TCT/AUA trinucleotide resulted in no cleaved product after 72 h (data not shown).

Since the maximum rate constant of approximately 1×10^{-2} h^{-1} was obtained in the presence of $MgCl_2$, with the duplexes forming a TA^{naph}T/AGA or TC^{naph}T/AUA trinucleotide, we performed RNA hydrolysis with $MnCl_2$ that efficiently provided the hydrolyzed fragment, as shown in Figure 2. Figure 5C shows that the reactions exhibited ~40 and ~70% of the cleaved RNA fragment only after 5 h. The rate constants (0.15 and 0.35 h^{-1}, respectively) were more than 15−30 times greater than that performed with $MgCl_2$, and the short reaction time significantly eliminated the occurrence of nonspecific hydrolysis (Figure 5D).

DISCUSSION

Mechanism of RNA Hydrolysis Induced by Base Pair Analogues. One of the most remarkable properties of the base pair analogues shown in Figure 1 is the ability to induce site-selective base flipping in a complementary strand. We performed nonenzymatic RNA hydrolysis to investigate the conformation and dynamics of the flipped-out ribonucleotide. The transesterification process results in the hydrolysis of an RNA phosphodiester linkage, and the reaction proceeds via an in-line attack mechanism in which the arrangement of the attacking 2′-hydroxyl group and the 5′-leaving oxygen atom of the phosphate group adopts an apical orientation (*24*). Watson−Crick base pairs are far from the in-line attack conformation, but an unconstrained nucleotide is transiently allowed to adopt the in-line arrangement (*25*, *26*), which allows us to probe the RNA structure (*27*−*29*).

We observed an exclusive site-selective RNA hydrolysis at the 3′-end of the ribonucleotide opposite deoxyadenosine and deoxycytidine derivatives in the presence of a divalent metal ion (Figures 2 and 3). It should be noted that the base pair analogues do not have the ability to catalyze RNA hydrolysis. Rather, the aromatic hydrocarbon group intercalation induces flipping of the

opposite ribonucleotide base into an extrahelical position susceptible to hydrolysis by a nucleophilic attack. The observations of no hydrolysis with an exchange-inert $[Co(NH_3)_6]^{3+}$ and faster hydrolysis in the presence of a metal ion with a lower pK_a based on the linear correlation with a slope close to −1 suggest specific base catalysis involving a metal-bound hydroxide ion. Manganese ion, having the lowest pK_a among the metal ions examined in this study, most efficiently cleaved the RNA, and the duplex sequence forming a TW_1T/AW_2A trinucleotide in the presence of $MnCl_2$ exhibited the highest reaction efficiency with minimum hydrolysis at nonspecific sites (Figure 5). Thus, the base pair analogues can be used for the site-selective cleavage of a target RNA.

Flexible Dynamics of the Flipped-Out Ribonucleotide. Specific base catalysis around neutral pH is extremely slow, and the reaction is partially limited by rearrangements in the in-line attack conformation (*25*, *26*). Although RNA hydrolysis induced by the base pair analogue was relatively slow, the rate was much faster than those of the unmodified duplexes forming a mismatch pair. According to the rate constant data indicated in Table 2 and Figure 5, there seems to be a limit to the hydrolysis rate in ranging from 1.5×10^{-3} to 3×10^{-3} h^{-1} in the presence of 10 mM $MgCl_2$ regardless of the types of base pair analogues and adjacent base pairs, with an exception of the TW_1T/AW_2A trinucleotide sequence. Li and Breaker reported the kinetics of specific base catalysis toward single-stranded chimeric DNA-RNA oligonucleotides and proposed an empirical equation that can predict the rate constant of specific base-catalyzed RNA hydrolyses of a structurally unconstrained ribonucleotide (*23*). According to the empirical equation, the rate constants of $1-3 \times 10^{-3}$ h^{-1} were established under our experimental conditions. Although a sodium ion was used in this study instead of a potassium ion, from which the empirical equation was established, the estimation of the rate constants was in agreement with the hydrolysis data obtained in this study. Therefore, the base pair analogues induce ribonucleotide base flipping of a structurally unconstrained phosphodiester linkage as much as ribonucleotides in a single-stranded state.

Intercalation of the Phenyl and Naphthyl Groups. The base flipping conformation is usually very unstable because it cannot maintain the integrity of a double-helical structure. The T_m values of duplexes containing a base pair analogue are somewhat smaller than those containing A/U and C/G base pairs but higher than the unmodified mismatch pairs at W_1/W_2 (Table 1). These results indicate that the energy cost for base flipping is at least partly compensated by the intercalation of the aromatic hydrocarbon group on base pair analogues. It is noted that our previous study using DNA duplexes containing an abasic site analogue demonstrated a high interaction energy by intercalating the aromatic rings in the absence of having a flipped-out base (*17*). The naphthyl group provides more stacking interaction than the phenyl group, which is evident from the higher T_m values of the duplexes containing A^{naph} (55.4−57.4 °C) compared to the values of those containing A^{phe} (52.4−53.2 °C). A stronger interaction by the naphthyl group (58.3−60.7 °C) than by the phenyl group (55.2−56.2 °C) is also indicated for deoxycytidine derivatives paired with A, C, or U. However, the ribonucleotide hydrolysis rates opposite A^{phe} or C^{phe} were similar to those opposite A^{naph} or C^{naph}, respectively. This observation suggests that base flipping by the stacking of the phenyl group is as efficient as that by the naphthyl group. Because the T_m values of the duplexes containing C^{phe} or C^{naph} are higher than the values of those containing A^{phe} or A^{naph}, it is possible that the stacking interaction of deoxycytidine derivatives is more efficient than that of deoxyadenosine derivatives. In fact, RNA hydrolyses mediated by the deoxycytidine derivatives were up to 4.2 times faster than that by the corresponding deoxyadenosine derivatives (Table 2).

Formation of Watson−Crick Base Pairs. The base pair analogues can form a base pair with the partner ribonucleotide in accordance with the Watson−Crick base pairing rule. The inability to form A^{phe}/U and A^{naph}/U base pairs indicates that an intercalation of the phenyl or naphthyl group is energetically more favorable than the base pairing between U and the adenine moiety. In contrast, either no or a small amount of the cleaved product was observed when G was located opposite C^{phe} or C^{naph}, indicating that C^{phe}/G and C^{naph}/G base pairs were formed through hydrogen bonds rather than a guanine flipping conformation. Unlike other mismatch pairs, the duplex stability was decreased via substitution of the naphthyl group for the phenyl group on the deoxycytidine derivative opposite G (Table 1). The same trend was also observed for the DNA/RNA duplexes forming different trinucleotide pairs (Table S1 of the Supporting Information) and the studies using a DNA duplex (*30*). Thus, it is likely that the larger hydrocarbon group is energetically unfavorable for the base pairing with G.

Although the reaction rate was relatively slow, the G residue located opposite C^{naph} was indeed hydrolyzed (Figures 5B and S3). This observation suggests a transient formation of the guanine flipping conformation, although the base pairing is a dominant conformation. It is likely that the stacking interaction of the naphthyl group on C^{naph} is sufficiently strong to compete with base pair formation with G, resulting in the easy adoption of a ribonucleotide base flipping conformation in equilibrium. The importance of the interaction energy on a ribonucleotide conformation was also indicated in the studies using I. Specifically, inosine formed a base pair with C through two hydrogen bonds that were weaker than the interaction energy of the C/G base pair but similar to that of the A/U base pair, which was evident from the T_m data (65.0, 70.8, and 63.0 °C for the duplexes containing C/I, C/G, and A/U pairs, respectively). The C^{phe}/G pair resulted in no cleaved RNA product, but the C^{phe}/I pair induced hydrolysis as observed for the A^{phe}/U pair. Thus, it is postulated that the stacking interaction of the phenyl group intercalation overcomes the base pair energy of A^{phe}/U or C^{phe}/I through two hydrogen bonds, but that this is not the case for the interaction energy of the three hydrogen bonds in the C^{phe}/G base pair. The amount of intercalation energy necessary to compete with base pair formation was also obtained when substituting the naphthyl group for the phenyl group. The T_m of the duplex containing the C^{naph}/I pair (58.4 °C), which is similar to the values of those containing C^{naph}/A, C^{naph}/C, and C^{naph}/U pairs (58.3−60.7 °C), is consistent with the I base flipping conformation. Hence, the base pair analogues can adopt a dual conformation in aromatic hydrocarbon group stacking and base pairing with a complementary base, depending on their interaction energy. A dual-conformational behavior is also observed during the DNA repair and DNA and RNA modification processes by enzymes that flip target bases out of the helical stack. It is suggested that the enzymes compensate for the energy cost of base flipping by intercalating the side chain of an amino acid and interactions with the flipped-out base (*5*) and that oxidized cytosine lesions are recognized by uracil DNA glycosylase in accordance with weakened base pair interactions (*11*). Similarly, the base pair

analogues can stabilize the base flipping conformation by the intercalation of the aromatic hydrocarbon group and can discriminate nucleotides in accordance with the base pair interaction energy, such as G from I, in which the base pair stability with cytosine was slightly different.

CONCLUSIONS

The base flipping conformation is found in DNA repair and DNA and RNA modification processes performed by enzymes. In addition, unpaired nucleotides are common RNA motifs, and the flipped-out bases can participate in RNA splicing and ribozyme reactions (*31*, *32*). The deoxyadenosine and deoxycytidine derivatives have the ability to intercalate their aromatic hydrocarbon groups into the helix and stabilize the base flipping conformation. The unusual conformation of a ribonucleotide was eventually hydrolyzed in the presence of a divalent metal ion as a result of specific base catalysis. From the hydrolysis experiments, unconstrained flexibility similar to that of single-stranded ribonucleotides was indicated. It is mentioned that the highly site-specific hydrolysis of an RNA strand arises from minimized perturbations of base pairs, including those adjacent to base pair analogues. In addition, the relatively high stability of a duplex with a short oligonucleotide has advantages for conducting studies of base flipping and nonenzymatic RNA hydrolysis.

It is important to know the energetics of the equilibrium between an intrahelical base stacking state and a flipped out state for the purpose of base flipping (*33*). However, the two conformations are usually far from equilibrium, and this is the barrier of base flipping research by experiments. The base pair analogues have the base moiety for base pairing that can compete with the aromatic hydrocarbon stacking. We suggest base pairing between the deoxycytidine derivatives and G, but not between the deoxyadenosine derivatives and U or between the deoxycytidine derivatives and I. The large stacking area of the naphthyl group was more likely to overcome the interaction energy of base pairing, even that of the C/G base pair. In contrast, alterations in the base pairs adjacent to a base pair analogue that changed the duplex stability and strength of the stacking interaction only slightly affected the hydrolysis rate. Hence, the ribonucleotide opposite the base pair analogues changes its conformation depending on the interaction energies of the aromatic group intercalation and base pairing through hydrogen bonds. Remarkably, this property arises from the fact that the two conformations are not far from the thermodynamic equilibrium; e.g., they differed in the interaction energy in response to a single hydrogen bond. Accordingly, the molecular design using a ureido linker that tethers an aromatic hydrocarbon group to a nucleobase would be useful for obtaining artificial nucleotides for investigating the base flipping under the equilibrium with base pairing. These artificial nucleotides can be used to investigate recognition mechanisms of DNA repair and DNA and RNA modification proteins and to estimate dynamics and energetics of the base flipping conformation involved in RNA folding motifs.

SUPPORTING INFORMATION AVAILABLE

Thermal melting curves and T_m values of DNA/RNA duplexes and amounts of the cleaved RNA fragment versus time. This material is available free of charge via the Internet at http://pubs.acs.org.

REFERENCES

1. Turner, D. H., Sugimoto, N., Kierzek, R., and Dreiker, S. D. (1987) Free energy increments for hydrogen bonds in nucleic acid base pairs. *J. Am. Chem. Soc. 109*, 3793–3784.
2. Bommarito, S., Peyret, N., and SantaLucia, J., Jr. (2000) Thermodynamic parameters for DNA sequences with dangling ends. *Nucleic Acids Res. 28*, 1929–1934.
3. Ohmichi, T., Nakano, S., Miyoshi, D., and Sugimoto, N. (2002) Long RNA dangling end has large energetic contribution to duplex stability. *J. Am. Chem. Soc. 124*, 10367–10372.
4. Moody, E. M., and Bevilacqua, P. C. (2003) Thermodynamic coupling of the loop and stem in unusually stable DNA hairpins closed by CG base pairs. *J. Am. Chem. Soc. 125*, 2032–2033.
5. Roberts, R. J., and Cheng, X. (1998) Base flipping. *Annu. Rev. Biochem. 67*, 181–198.
6. Yi-Brunozzi, H. Y., Stephens, O. M., and Beal, P. A. (2001) Conformational changes that occur during an RNA-editing adenosine deamination reaction. *J. Biol. Chem. 276*, 37827–37833.
7. Sankpal, U. T., and Rao, D. N. (2002) Structure, function, and mechanism of HhaI DNA methyltransferases. *Crit. Rev. Biochem. Mol. Biol. 37*, 167–197.
8. Gelfand, C. A., Plum, G. E., Grollman, A. P., Johnson, F., and Breslauer, K. J. (1998) Thermodynamic consequences of an abasic lesion in duplex DNA are strongly dependent on base sequence. *Biochemistry 37*, 7321–7327.
9. Sagi, J., Guliaev, A. B., and Singer, B. (2001) 15-mer DNA duplexes containing an abasic site are thermodynamically more stable with adjacent purines than with pyrimidines. *Biochemistry 40*, 3859–3868.
10. Hazel, R. D., Tian, K., and de Los Santos, C. (2008) NMR solution structures of bistranded abasic site lesions in DNA. *Biochemistry 47*, 11909–11919.
11. Krosky, D. J., Schwarz, F. P., and Stivers, J. T. (2004) Linear free energy correlations for enzymatic base flipping: How do damaged base pairs facilitate specific recognition? *Biochemistry 43*, 4188–4195.
12. Lipscomb, L. A., Zhou, F. X., Presnell, S. R., Woo, R. J., Peek, M. E., Plaskon, R. R., and Williams, L. D. (1996) Structure of DNA-porphyrin complex. *Biochemistry 35*, 2818–2823.
13. Morales-Rojas, H., and Kool, E. T. (2002) A porphyrin C-nucleoside incorporated into DNA. *Org. Lett. 4*, 4377–4380.
14. Smirnov, S., Matray, T. J., Kool, E. T., and de los Santos, C. (2002) Integrity of duplex structures without hydrogen bonding: DNA with pyrene paired at abasic sites. *Nucleic Acids Res. 30*, 5561–5569.
15. Tuma, J., Connors, W. H., Stitelman, D. H., and Richert, C. (2002) On the effect of covalently appended quinolones on termini of DNA duplexes. *J. Am. Chem. Soc. 124*, 4236–4246.
16. David, A., Bleimling, N., Beuck, C., Lehn, J. M., Weinhold, E., and Teulade-Fichou, M. P. (2003) DNA mismatch-specific base flipping by a bisacridine macrocycle. *ChemBioChem 4*, 1326–1331.
17. Nakano, S., Uotani, Y., Uenishi, K., Fujii, M., and Sugimoto, N. (2005) DNA base flipping by a base pair-mimic nucleoside. *Nucleic Acids Res. 33*, 7111–7119.
18. Nakano, S., Uotani, Y., Uenishi, K., Fujii, M., and Sugimoto, N. (2005) Site-selective RNA cleavage by DNA bearing a base pair-mimic nucleoside. *J. Am. Chem. Soc. 127*, 518–519.
19. Richard, R. G. (1975) in Handbook of Biochemistry and Molecular Biology: Nucleic Acids (Fasman, G. D., Ed.) 3rd ed., Vol. 1, p 597, CRC Press, Cleveland, OH.
20. Puglisi, J. D., and Tinoco, I., Jr. (1989) Absorbance melting curves of RNA. *Methods Enzymol. 180*, 304–325.
21. Sugimoto, N., Nakano, M., and Nakano, S. (2000) Thermodynamics-structure relationship of single mismatches in RNA/DNA duplexes. *Biochemistry 39*, 11270–11281.
22. Jencks, W. P. (1969) Catalysis in Chemistry and Enzymology , pp 163−242, John Wiley & Sons, Inc., New York.
23. Li, Y., and Breaker, R. R. (1999) Kinetics of RNA degradation by specific base catalysis of transesterification invoving 2′-hydrolyl group. *J. Am. Chem. Soc. 121*, 5364–5372.
24. Zhou, D. M., and Taira, K. (1998) The hydrolysis of RNA: From theoretical calculations to the hammerhead ribozyme-mediated cleavage of RNA. *Chem. Rev. 98*, 991–1026.
25. Soukup, G. A., and Breaker, R. R. (1999) Relationship between internucleotide linkage geometry and the stability of RNA. *RNA 5*, 1308–1325.
26. Tereshko, V., Wallace, S. T., Usman, N., Wincott, F. E., and Egli, M. (2001) X-ray crystallographic observation of "in-line" and "adjacent" conformations in a bulged self-cleaving RNA/DNA hybrid. *RNA 7*, 405–420.

27. Winkler, W. C., Cohen-Chalamish, S., and Breaker, R. R. (2002) An mRNA structure that controls gene expression by binding FMN. *Proc. Natl. Acad. Sci. U.S.A. 99*, 15908–15913.
28. Gopinath, S. C., Matsugami, A., Katahira, M., and Kumar, P. K. (2005) Human vault-associated non-coding RNAs bind to mitoxantrone, a chemotherapeutic compound. *Nucleic Acids Res. 33*, 4874–4881.
29. Espinoza, C. A., Goodrich, J. A., and Kugel, J. F. (2007) Characterization of the structure, function, and mechanism of B2 RNA, an ncRNA repressor of RNA polymerase II transcription. *RNA 13*, 583–596.
30. Miyata, K., Tamamushi, R., Ohkubo, A., Taguchi, H., Seio, K., and Sekine, M. (2004) Synthesis and hybridization affinity of oligodeoxyribonucleotides incorporating 4-*N*-(*N*-arylcarbamoly)deoxycytidine derivatives. *Tetrahedron Lett. 45*, 9365–9368.
31. Andersen, A. A., and Collins, R. A. (2000) Rearrangement of a stable RNA secondary structure during VS ribozyme catalysis. *Mol. Cell 5*, 469–478.
32. Reiter, N. J., Blad, H., Abildgaard, F., and Butcher, S. E. (2004) Dynamics in the U6 RNA intramolecular stem-loop: A base flipping conformational change. *Biochemistry 43*, 13739–13747.
33. Barthel, A., and Zacharias, M. (2006) Conformational transitions in RNA single uridine and adenosine bulge structures: A molecular dynamics free energy simulation study. *Biophys. J. 90*, 2450–2462.